Journal of Translational Medicine

RESEARCH

Open Access

Interferon regulatory factor 7 alleviates the experimental colitis through enhancing IL-28A-mediated intestinal epithelial integrity

Furong Qing[1†], Hongbo Tian[2†], Biyao Wang[3,4†], Bingyu Xie[1], Lina Sui[1], Xiaoyan Xie[1], Wenji He[1], Tiansheng He[1], Yumei Li[1], Liangmei He[5], Qin Guo[3,4*] and Zhiping Liu[1,6*]

Abstract

Background The incidence of inflammatory bowel disease (IBD) is on the rise in developing countries, and investigating the underlying mechanisms of IBD is essential for the development of targeted therapeutic interventions. Interferon regulatory factor 7 (IRF7) is known to exert pro-inflammatory effects in various autoimmune diseases, yet its precise role in the development of colitis remains unclear.

Methods We analyzed the clinical significance of IRF7 in ulcerative colitis (UC) by searching RNA-Seq databases and collecting tissue samples from clinical UC patients. And, we performed dextran sodium sulfate (DSS)-induced colitis modeling using WT and *Irf7*$^{-/-}$ mice to explore the mechanism of IRF7 action on colitis.

Results In this study, we found that IRF7 expression is significantly reduced in patients with UC, and also demonstrated that *Irf7*$^{-/-}$ mice display heightened susceptibility to DSS-induced colitis, accompanied by elevated levels of colonic and serum pro-inflammatory cytokines, suggesting that IRF7 is able to inhibit colitis. This increased susceptibility is linked to compromised intestinal barrier integrity and impaired expression of key molecules, including Muc2, E-cadherin, β-catenin, Occludin, and Interleukin-28A (IL-28A), a member of type III interferon (IFN-III), but independent of the deficiency of classic type I interferon (IFN-I) and type II interferon (IFN-II). The stimulation of intestinal epithelial cells by recombinant IL-28A augments the expression of Muc2, E-cadherin, β-catenin, and Occludin. The recombinant IL-28A protein in mice counteracts the heightened susceptibility of *Irf7*$^{-/-}$ mice to colitis induced by DSS, while also elevating the expression of Muc2, E-cadherin, β-catenin, and Occludin, thereby promoting the integrity of the intestinal barrier.

Conclusion These findings underscore the pivotal role of IRF7 in preserving intestinal homeostasis and forestalling the onset of colitis.

Keywords IRF7, Colitis, IL-28A, Epithelial barrier, Interferon

†Furong Qing, Hongbo Tian and Biyao Wang are co-first authors.

*Correspondence:
Qin Guo
guoq83@mail.sysu.edu.cn
Zhiping Liu
Zhiping.Liu@gmu.edu.cn
Full list of author information is available at the end of the article

© The Author(s) 2024. **Open Access** This article is licensed under a Creative Commons Attribution-NonCommercial-NoDerivatives 4.0 International License, which permits any non-commercial use, sharing, distribution and reproduction in any medium or format, as long as you give appropriate credit to the original author(s) and the source, provide a link to the Creative Commons licence, and indicate if you modified the licensed material. You do not have permission under this licence to share adapted material derived from this article or parts of it. The images or other third party material in this article are included in the article's Creative Commons licence, unless indicated otherwise in a credit line to the material. If material is not included in the article's Creative Commons licence and your intended use is not permitted by statutory regulation or exceeds the permitted use, you will need to obtain permission directly from the copyright holder. To view a copy of this licence, visit http://creativecommons.org/licenses/by-nc-nd/4.0/.

New and noteworthy

The present study demonstrates that IRF7 exerts an inhibitory effect on colitis pathogenesis by inducing the expression of Muc2, E-cadherin, β-catenin, and Occludin via upregulation of IL-28A, thereby enhancing the integrity and functionality of the intestinal epithelial barrier. These findings provide novel preclinical evidence for the potential therapeutic targeting of IRF7 in patients with IBD, representing a significant advancement in the field.

Introduction

IBD encompasses Crohn's disease (CD) and UC, is a persistent and relapsing inflammatory disorder of the gastrointestinal tract, characterized by aberrant immune responses to microbial and environmental factors in genetically susceptible individuals. The pathogenesis of IBD is acknowledged to involve the interplay between intestinal microorganisms or microbial products, intestinal epithelial cells, and the local immune system, which leads to an aberrant mucosal immune response and the subsequent overproduction of inflammatory cytokines [1]. Several investigations have demonstrated that the degradation of the colonic mucus layer is particularly evident in individuals with IBD, and the extent of intestinal epithelial barrier disruption is directly correlated with an imbalance of inflammatory cytokines [2].

The generation of inflammatory cytokines necessitates the activation of transcription factors, such as nuclear factor kappa-B (NF-κB) and interferon regulatory factors (IRFs). NF-κB serves as a crucial regulator of transcription for inflammatory cytokines and chemokines, and is highly activated during the host immune response. Its primary function is to promote inflammation, which can result in tissue damage, or to maintain tissue homeostasis [3]. Various studies have demonstrated that the administration of antisense oligonucleotides of NF-κB p65 or peptides that bind to NEMO and inhibit Iκκ can effectively reduce the severity of chemically induced and IL-10 deficiency induced murine colitis [4, 5]. Additionally, the nuclear hormone receptor Rev-erbα has been shown to mitigate colitis by inhibiting NF-κB p65 transcription and NLRP3 activation [6].

Interferon regulatory factors (IRFs) are a versatile family of transcription factors that encompass IRF1-9. These factors regulate the production of interferons (IFNs) through their DNA binding domains and are extensively involved in innate and acquired immunity [7]. IRF7, in particular, plays a direct role in inducing the production of IFN-I and IFN-III (Interferon-lambda, IFN-λ), but not IFN-II (Interferon-gamma, IFN-γ) [8–10]. IFN-I, which includes IFN-α and IFN-β, and IFN-III, which includes IL-29 (IFN-λ1), IL-28A (IFN-λ2), and IL-28B (IFN-λ3), are crucial factors in the antiviral and various inflammatory responses. Although sharing similarities in their activation pathways, IFN-I and IFN-III exhibit distinct functions. Specifically, both IFN-I and IFN-III are capable of inducing the expression of interferon-stimulated genes (ISGs), suppressing cell proliferation, and inhibiting cell death [11–13]. Moreover, the absence of both IFN-I and IFN-III receptors in mice has been shown to result in heightened barrier destruction and increased susceptibility to colitis [14]. However, IFN-I has been observed to primarily act on cells in the lamina propria, while IFN-III predominantly targets epithelial cells [15, 16]. Furthermore, the kinetics and magnitude of ISG induction in response to IFN-I and IFN-III may differ, as previously noted [17].

IRF7 and IRF3, which exhibit high structural homology, serve as major mediators of IFN-I induction downstream of various pattern recognition receptors (PRRs), including Toll-like receptors, AIM2-like receptors, and RIG-I-like receptors [18]. However, their expression patterns differ, with IRF3 being ubiquitously expressed in many resting cells, while IRF7 is expressed at low levels in the absence of stimulation [19]. Additionally, IRF7 can function as both a homodimer and heterodimer with IRF3 [20].

Prior research has demonstrated the widespread involvement of IRF7 in inflammatory diseases. Specifically, IRF7 activation has been found to facilitate macrophage inflammation and contribute to diabetic atherosclerosis [21]. Additionally, activated IRF7 in plasmacytoid dendritic cells has been implicated in the promotion of experimental autoimmune pancreatitis [22]. Furthermore, certain investigations suggest that IRF7 transcriptionally upregulates chemoattractant protein-1 (MCP-1) mRNA levels in adipocyte monocytes, potentially playing a role in obesity-associated adipose tissue inflammation [23]. Our recent research findings indicate that the activation of mTORC1 and inhibition of autophagy by IRF3 and IRF7 exacerbate pulmonary inflammation induced by diesel exhaust particles [24].

Conversely, a previous study has demonstrated that IRF3 plays a role in mitigating colitis by regulating the production of thymic stromal lymphopoietin (Tslp) gene mediated by microbiota [25]. To date, a direct evaluation of the involvement of IRF7 in the pathogenesis of colitis has not been conducted, and the precise mechanism by which IRF7 modulates colitis development remains unclear.

The present investigation sought to elucidate the specific contribution of IRF7 to colitis development by utilizing *Irf7*$^{-/-}$ mice. Our findings indicate that *Irf7*$^{-/-}$ mice exhibit heightened susceptibility to DSS-induced colitis and impaired intestinal integrity. The administration of recombinant IL-28A protein reversed this phenotype and

restored intestinal integrity. Consistently, IL-28A levels in sera of UC patients were significantly lower than those in sera of healthy controls. This investigation highlights the significant role played by IRF7-induced IL-28A in the preservation of intestinal epithelial integrity.

Materials and methods

Human specimens and data

To assess the association between IRF7 expression and UC patients, we retrieved previously published publicly available transcriptional data with the archive number GSE105074. Then, colon tissue sections (lesions and non-lesions) from 16 patients with chronic persistent and acute fulminant UC were obtained from the Sixth Affiliated Hospital of Sun Yat-sen University (Guangzhou, Guangdong). After excluding samples with missing clinical information, suffering from underlying diseases, and after follow-up or medication, 32 diseased/non-diseased tissue slides from patients were obtained.

Mice

The *Irf7*$^{-/-}$ mice and corresponding wild-type (WT) mice were generously provided by Dr. Xiaopeng Qi from the Kunming Institute of Animal Science, Chinese Academy of Sciences, Kunming, Yunnan, China and were previously described [24]. The present study employed mouse strains of C57BL/6 background, which were selected based on age (6–8 weeks old) and gender (male or female) matching. The mice were housed in the SPF facility of the Experimental Animal Center of Gannan Medical University, Ganzhou, Jiangxi, China, under conditions that simulated normal day and night cycles, and were provided with ad libitum access to sterile drinking water. The Ethics Committee of Gannan Medical University granted approval for the study.

The establishment of experimental colitis

The survival experiments were conducted by administering 4% DSS to the mice via drinking water for a period of 5 days, followed by normal drinking water without DSS. The survival of mice was monitored. Additionally, experimental colitis was induced in mice by administering 3% dextran sodium sulfate (DSS, Molecular mass 36–40 kDa; MP Biologicals) in their drinking water for a period of five days, followed by normal drinking water without DSS for an additional three days. Body weights were monitored and recorded throughout the experiment. On the eighth day following the initial DSS exposure, mice were sacrificed and colon tissues were collected for analysis. Colon lengths were measured and clinical scores for stool consistency and rectal bleeding were determined using previously established methods [26]. The methodology employed in this study involved the determination of stool scores, which were assigned based on the following criteria: 0 denoted well-formed pellets, 1 indicated semi-formed stools that did not adhere to the anus, 2 represented semiformed stools that adhered to the anus, and 3 signified liquid stools that adhered to the anus. Bleeding scores were also determined, with 0 indicating the absence of blood as detected by hemoccult (Beckman Coulter), 1 indicating a positive hemoccult result, 2 indicating the presence of blood traces in stool that were visible, and 3 indicating gross rectal bleeding.

Histopathological analysis

Colonic tissues were collected and subjected to formalin fixation for 24 h. The fixed tissues were then embedded in paraffin, sectioned to a thickness of 5 μm, and stained with hematoxylin and eosin (H&E). The resulting sections were evaluated for histopathological scoring based on the extent of inflammatory infiltration, ulceration, mucosal hyperplasia, and lesion severity. The inflammation scoring criteria were categorized as follows: normal (score of 0), inflammation infiltration to the lamina propria (score of 1), inflammation infiltration to the submucosa (score of 2), and inflammation infiltration to the entire layer (score of 3). Ulcer degree score: normal = 0, 1–2 ulcers and less than 20 crypts = 1, 1–4 ulcers or 20–40 crypts = 2, greater than 4 ulcers or 40 crypts = 3. Mucosal hyperplasia degree: normal = 0, 2–3 times thickness = 1, 2- threefold thickness, epithelial staining, cupped cell reduction or glandular branching = 2, fourfold thickness, epithelial staining, cupped cell reduction, nuclear division or glandular branching = 3. Extent of lesion: 0 = 0, 0–30% = 1, 31%-70% = 2, greater than 71% = 3. The histopathology score of the section is the sum of the four scores, with a maximum score of 12. Goblet cells were stained by PAS using PAS staining solution kit (Servicebio, Wuhan, China) following the manufacturers' instructions.

RT-qPCR

The extraction of colonic RNA was performed using TRIzol, followed by cDNA transcription using a cDNA reverse transcription kit (TaKaRa AJG1624A) as per the manufacturer's instructions. The detection of gene expression was carried out using SYBR Green fluorescence quantification reagent (Applied Biosystems), with primer sequences listed in Supplemental Table 1 and Supplemental Table 2.

ELISA

The quantification of cytokines in colon tissue homogenate, serum, or cell supernatants was determined by ELISA. The colon tissues were homogenized in RIPA lysis

buffer containing PMSF, protease inhibitor, and phosphatase inhibitor using a cryogenic freeze grinder (Jingxin, Shanghai, China). After centrifugation, both serum and cell supernatants were collected. The ELISA kit information for IL-6 (Signosis, EA-2206), TNF-α (Signosis, EA-2203), IL-1β (Signosis, EA-2508), IFN-α (Jingmei, JM-02649M1), IFN-β (Jingmei, JM-02407M1), IFN-γ (Cloud-Clone, SEA049Mu), IL-33 (Elabscience, E-EL-M2642c), IL-28A (Cloud-Clone, SEB689Mu), and IL-28B (Cloud-Clone, MEC028Mu) were listed. IL-28A in sera from UC patients and healthy individuals were determined by IL-28A ELISA kits (Cloud-Clone, SEB689Hu). The ELISA procedures were carried out in accordance with the manufacturers' instructions.

In vivo intestinal permeability measurement

Intestinal permeability was assessed using the FITC-dextran assay, as previously described [27]. Following an overnight fast, mice were administrated with FITC-dextran (3–5 kDa, Sigma-Aldrich, BCBW4673, 60 mg/100 g body weight) orally, three hours prior to necropsy. Subsequently, the mice were sacrificed and serum samples were collected. The concentration of FITC-dextran in the serum was determined using fluorescence spectrophotometry (490/520 nm).

Western-blot

The samples were lysed using RIPA lysis buffer containing PMSF, protease inhibitor, and phosphatase inhibitor. To quantify protein using the BCA method, the samples were diluted to a uniform concentration through the addition of 4X Loading buffer. The resulting protein samples (20 μg/well) were then separated through electrophoresis on a 10% SDS-PAGE gel and transferred onto a PVDF membrane. Following a 1-h blocking period in 5% milk, the membranes were incubated overnight at 4 °C in a shaker with primary antibodies, including β-actin (Proteintech, 66,009–1-Ig), Muc2 (abcam, ab272692), E-cadherin (CST, 3195), β-catenin (CST, 8480 s), and Occludin (abcam, ab216327). The membranes underwent a washing procedure followed by incubation with HRP-labeled secondary antibody (1:5000). Subsequently, they were developed using enhanced chemiluminescence (ECL) contrast solution. Finally, protein quantification was conducted by measuring the absorbance of the protein bands through Image J software.

Immunofluorescence analysis

The colon tissues were obtained, formalin-fixed, paraffin-embedded, sectioned (5 μm). Following this, they were dewaxed and antigen-retrieved. Slides were incubated in 3% bovine serum albumin (BSA) at room temperature for 1 h, followed by overnight incubation at 4 °C with primary antibodies, including Muc2 (1:500, abcam, ab272692), E-cadherin (1:1000, CST, 3195), β-catenin (1:200, CST, 8480 s), or Occludin (1:100, abcam, ab216327). Subsequently, slides treated with secondary antibody (1:200) labeled with fluorescence (DyLight 488) for 1 h at room temperature. After washing, anti-fluorescence attenuation blocker (containing DAPI) was added dropwise, and the slides were analyzed using the Panoramic Tissue Cell Quantification System (TissueFAXS Plus, TissueGnostics, Austria).

Immunohistochemistry analysis

The colon tissues were obtained, formalin-fixed, paraffin-embedded, sectioned (5 μm). Following this, they were dewaxed and antigen-retrieved. Slides were incubated in 3% H_2O_2 at room temperature for 20 min, followed by incubation in 10% BSA at room temperature for 30 min, and then incubated overnight at 4 °C with primary antibody (IRF7 (1:200, invitrogen, PA5-102,832)). Subsequently, slides were incubated with enzyme-labeled goat anti-mouse/rabbit IgG polymer (ZSGB-BIO, PV-6000) at room temperature for 1 h. After PBS washing, DAB color development solution (ZSGB-BIO, ZLI-9019) was added dropwise. Hematoxylin staining, dehydration, transparency, and sealing.

Slides were analyzed using the Panoramic Tissue Cell Quantification System (TissueFAXS Plus, TissueGnostics, Austria). Scoring criteria: the intensity of expression is categorized as low (1 point), medium (2 points) and high (3 points), and the range of expression is categorized as < 10% (1 point), 10–50% (2 points) and > 50% (3 points). The expression range was divided into < 10% (1 point), 10–50% (2 points) and > 50% (3 points), and the expression intensity multiplied by the expression range was the protein expression level of the tissue.

Stimulation of bone marrow-derived macrophages (BMDM)

BMDM were procured from the femur and tibia of mice and cultured in a medium supplemented with L929 supernatant, as previously described [27]. At specific time intervals, BMDM were stimulated with 1 μg poly(I:C) (1 μg/μL) (Peprotech, 250–33), and the cell supernatants were collected post-stimulation.

Cell culture and treatments

The human colorectal cancer epithelial cell lines HCT116 and Caco2 were procured from the American Type Culture Collection (ATCC, Manassas, VA, USA). HCT116 cells were cultured in 1640 medium (VivaCell, C3010-0500) supplemented with 10% inactivated fetal bovine serum (FBS) (VivaCell, C04001-500) and 1% penicillin–streptomycin Liquid (100x) (Solarbio, P1400). Caco2 cells were cultured in MEM medium (Procell, PM150410) supplemented with 20% inactivated fetal bovine serum (FBS) (VivaCell,

C04001-500) and 1% penicillin–streptomycin Liquid (100x) (Solarbio, P1400). The cells were seeded at a density of 5×10^5 cells/well in 12-well plates. Subsequently, 1 μg of the pcDNA3.1-IRF7 plasmid, which was constructed for overexpression of IRF7, was combined with the transfection reagent PEI (polyethylenimine) to transfect HCT116 cells. The control group, on the other hand, was transfected with 1 μg of PRK mixed with PEI and incubated for 24 h. The efficiency of IRF7 transfection was assessed using the RT-qPCR method. Following this, the HCT116 cells were stimulated with 1 μg of poly(I:C) for 3 h, and subsequently collected for RT-qPCR analysis. Additionally, HCT116 and Caco2 cells were treated with 100 ng and 300 ng of IL-28A recombinant protein (PeproTech, 250–33), respectively.

In vivo injection of recombinant IL-28A

On the fifth day following DSS treatment, *Irf7*$^{-/-}$ mice were administered intraperitoneal injection of IL-28A recombinant protein (2 μg/mice, PeproTech, 250–33) or 1×PBS. Daily recordings were made of body weight, fecal viscosity score, and rectal bleeding score. On the eighth day, colonic tissues and sera were collected from the mice to measure colon length, the concentration of FITC-dextran, IL-28A, and other relevant proteins at three days post-injection.

Statistical analysis

Data analysis was conducted using Prism 8.0 software and expressed as mean ± s.e.m. The Kaplan–Meier test was utilized to analyze group survival rates. The study utilized a two-way ANOVA to assess the differences among multiple groups with two factors, and a student's *t* test was employed for comparisons between two groups. $P<0.05$ was considered statistically significant.

Results

Irf7$^{-/-}$ mice show enhanced susceptibility to DSS-induced colitis

To investigate the role of IRF7 in the host resistance to colitis, we compared gene expression differences in RNA-seq data from colon tissues of healthy individuals and UC patients by reviewing databases. The expression of IRF7 was significantly reduced in UC patients (Fig. 1A) (GSE105074). To further validate the role of IRF7 in colitis, we collected colon tissue sections (lesions and non-lesions) from 16 patients with chronic persistent and acute fulminant UC at the Sixth Affiliated Hospital of Sun Yat-sen University. It was likewise found by immunohistochemical staining that IRF7 expression was significantly reduced in UC patients (Fig. 1B, C). This suggests that IRF7 may have an important role in the development of UC. We then modeled DSS-induced colitis in WT mice. It was found that IRF7 expression was significantly downregulated in mice that had consumed DSS compared to mice that had not consumed DSS (Fig. 1D).

In this regard, we performed the further investigation to determine the role of IRF7 in the development of colitis by subjecting *Irf7*$^{-/-}$ mice and corresponding WT mice to DSS-induced colitis. Survival rates were monitored in mice treated with 4% DSS in their drinking water. Results showed that 82.6% (19/23) of *Irf7*$^{-/-}$ mice died within 10 days, while 33.3% (5/15) of WT mice died (Fig. 1E). Subsequently, an assessment was conducted on mice treated with 3% DSS to determine their increased susceptibility to DSS-induced colitis in *Irf7*$^{-/-}$ mice. Notably, *Irf7*$^{-/-}$ mice exhibited a significant decline in body weight on day 6, 7, and 8 following the initiation of DSS treatment, as compared to WT mice (Fig. 1F). Furthermore, *Irf7*$^{-/-}$ mice demonstrated elevated scores for fecal viscosity and rectal bleeding, surpassing those of DSS-treated WT mice (Fig. 1G, H). Colon shortening is a primary characteristic of DSS-induced colitis, and on day 8 after the initiation of DSS treatment, mice were sacrificed for the evaluation of colon length. The present study revealed that the colons of *Irf7*$^{-/-}$ mice exhibited a statistically significant reduction in length when compared to those of WT mice (Fig. 1I). Additionally, the colons of *Irf7*$^{-/-}$ mice displayed a dark red coloration, along

(See figure on next page.)

Fig. 1 *Irf7*$^{-/-}$ mice show enhanced susceptibility to DSS-induced colitis. **A** *Irf7* mRNA expression in colonic tissues of UC patients compared to healthy individuals. **B** Immunohistochemical staining to compare IRF7 levels in diseased and non-diseased colonic tissues from UC patients, with a scale bar of 20 μm. **C** Immunohistochemical staining scores. **D** RT-qPCR to detect *Irf7* expression in colonic tissues of WT mice drinking/not drinking (n = 11) 3% DSS. **E** The survival rates of wild-type (WT) mice (n = 15) and *Irf7*$^{-/-}$ mice (n = 23) were assessed following treatment with 4% DSS. **F** The change in body weight, **G** stool consistency scores, **H** bleeding scores, and **I** colon length of both WT and *Irf7*$^{-/-}$ mice were measured on day 8 after treatment with 3% DSS. **J** Representative images of the colons from **I** were obtained. **K** The histological scores of the colon on day 8 were determined. **L** Representative images of haematoxylin and eosin (H&E) staining of the distal colon on day 8 were captured, with a scale bar of 100 μm. In (**F-I**, **K**), data were collected from WT (n = 5) and *Irf7*$^{-/-}$ (n = 5) mice. The experiment was independently repeated three times. The data presented in (**A**, **C**–**I**, **K**) are expressed as the mean ± s.e.m. NS, not significant, *$P<0.05$, **$P<0.01$, ***$P<0.001$, ****$P<0.0001$. Unpaired two-tailed student's *t*-test **(A**, **D**, **I**, **K),** paired two-tailed student's *t*-test (**C**), Log-rank (Mantel-Cox) test (**E**), and two-way ANOVA with Holm-Sidak's multiple comparisons test (**F–H**)

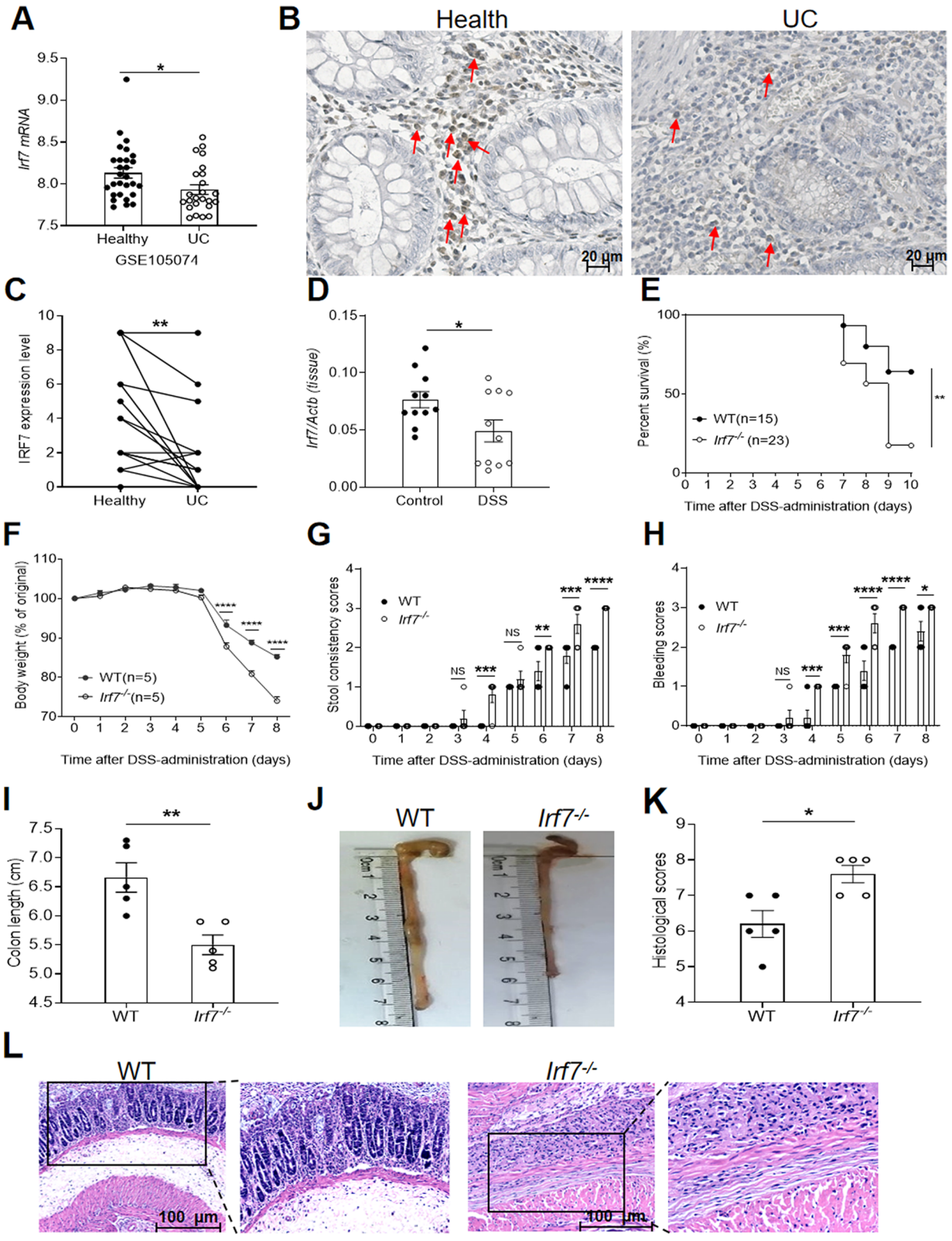

Fig. 1 (See legend on previous page.)

with a swollen and hemorrhagic intestinal wall, which is indicative of colitis (Fig. 1J). Furthermore, histological examination of the colons of *Irf7*$^{-/-}$ mice demonstrated a higher incidence of histological lesions, characterized by the loss of crypt structure in colonic tissue and the presence of ulcers, when compared to WT mice (Fig. 1K, L). These findings suggest that IRF7 can inhibit DSS-induced colitis.

Increased levels of IL-6, TNF-α, and IL-1β in *Irf7*$^{-/-}$ mice during colitis development

During the progression of colitis, the compromised intestinal barrier may facilitate the infiltration of pathogenic microorganisms, which in turn activate transcription factors such as IRF7 and stimulate the production of pro-inflammatory cytokines [28]. Among these cytokines, IL-6, TNF-α, and IL-1β are recognized as key mediators

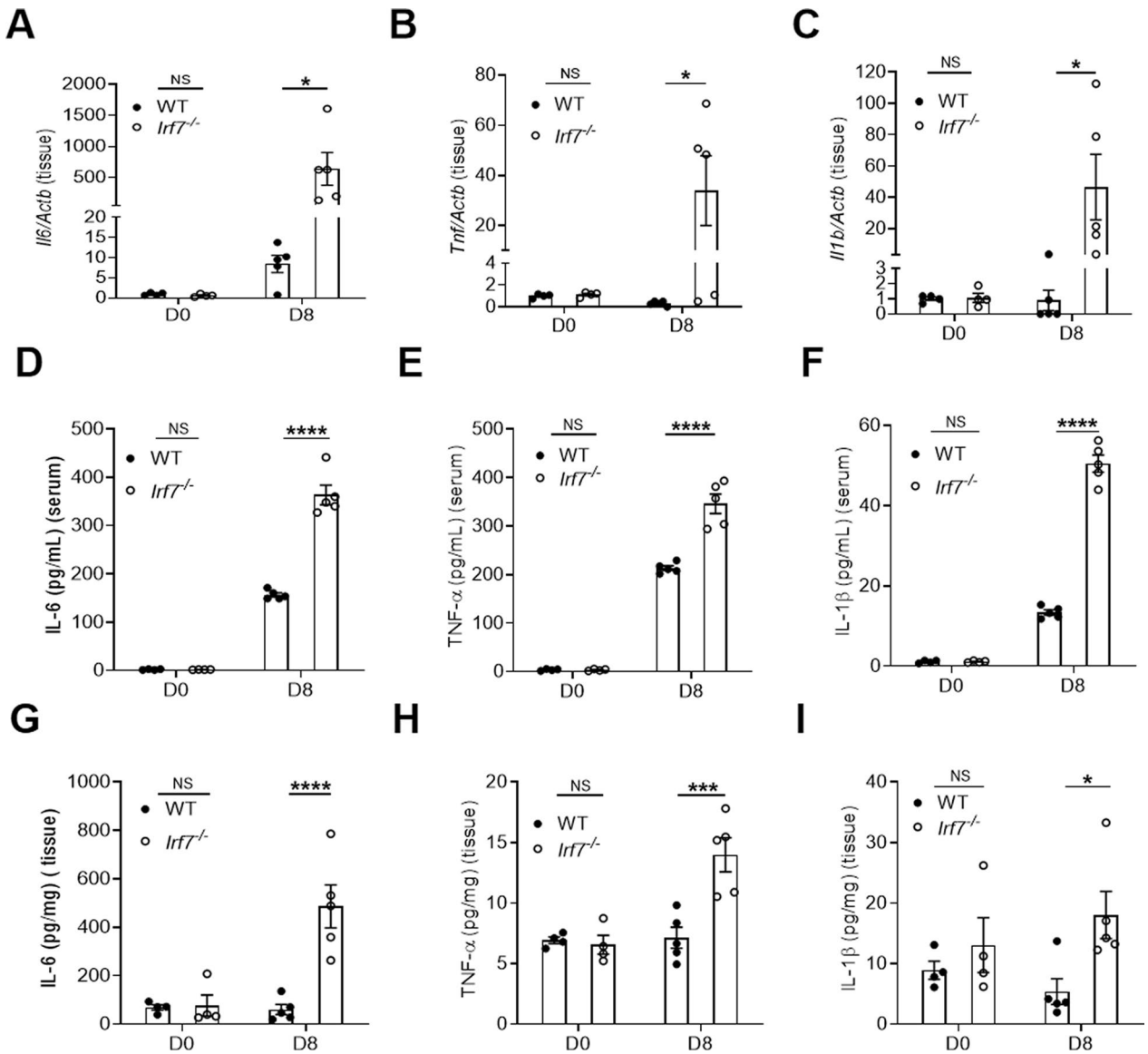

Fig. 2 *Irf7*$^{-/-}$ mice have higher expression levels of inflammatory cytokines than WT mice in DSS-induced colitis. WT and *Irf7*$^{-/-}$ mice were administered 3% DSS, and on days 0 and 8, sera and colons were collected. The expression of colonic inflammatory cytokines at the gene and protein levels was quantified using RT-qPCR and ELISA, respectively, while the protein levels of serum inflammatory cytokines were measured using ELISA. Specifically, the colonic gene expression of (**A**) *Il6*, **B** *Tnf*, and **C** *Il1b*, serum protein levels of **D** IL-6, **E** TNF-α, and **F** IL-1β, and colonic protein levels of **G** IL-6, **H** TNF-α, and **I** IL-1β were assessed. The sample sizes for each group at each time point were as follows: D0: WT (n = 4), *Irf7*$^{-/-}$ (n = 4) and D8: WT (n = 5), *Irf7*$^{-/-}$ (n = 5). The data are expressed as the mean ± s.e.m. NS, not significant, *$P < 0.05$, **$P < 0.01$, ***$P < 0.001$, ****$P < 0.0001$. Two-way ANOVA with Holm-Sidak's multiple comparisons test (**A-I**)

in the pathogenesis of inflammatory disorders. In this study, we employed RT-qPCR to assess the expression levels of Il6, Tnf, and Il1b in colonic tissues of Irf7$^{-/-}$ mice on day 0 and 8 after 3% DSS treatment. Our results revealed a significant upregulation of these genes in the aforementioned tissues on day 8, in comparison with WT mice (Fig. 2A–C). In accordance with these observations, the levels of serum and colonic IL-6, TNF-α, and IL-1β secretion in Irf7$^{-/-}$ mice were significantly elevated compared to WT mice on day 8, but not on days 0 (Fig. 2D-I). The findings of this study indicate that a deficiency in IRF7 leads to an increase in the production of pro-inflammatory cytokines, such as IL-6, TNF-α, and IL-1β, in DSS-induced colitis, thereby exacerbating both local and systemic inflammation.

The epithelial integrity and the expression level of barrier relevant genes are decreased in *Irf7*$^{-/-}$ mice during colitis development

Notably, intestinal permeability can be exacerbated by various external factors during the development of IBDs, and has been observed in asymptomatic patients years prior to the onset of clinical symptoms [29, 30]. In order to examine the potential impact of IRF7 on the permeability of intestinal epithelial cells, we orally administered FITC-dextran to both non-DSS-treated and DSS-treated WT and *Irf7*$^{-/-}$ mice. After three hours, we collected serum samples and quantified the concentration of FITC-dextran using fluorescence spectrophotometry. Our findings indicate that the values of FITC-dextran were comparable between WT mice and *Irf7*$^{-/-}$ mice without DSS treatment. This suggests that the deletion of *Irf7* alone does not have an effect on the function of the intestinal epithelial barrier. However, the results of WT mice and *Irf7*$^{-/-}$ mice treated with DSS showed a significant increase in FITC-dextran values of *Irf7*$^{-/-}$ mice compared with WT mice. This implies that the absence of *Irf7* can substantially enhance intestinal permeability in DSS-induced colitis (Fig. 3A). Consequently, the capacity of IRF7 to suppress DSS-induced colitis may be attributed, at least partially, to its role in preserving the integrity of the intestinal epithelial barrier.

Furthermore, we assessed the pertinent cytokines that are associated with the maintenance of epithelial integrity. IL-33 has the potential to stimulate epithelial repair and restitution, thereby enhancing gut mucosal healing during DSS-induced colitis [31]. The ELISA results revealed that there was no statistically significant difference in the secretion of IL-33 in colonic tissues of *Irf7*$^{-/-}$ mice when compared to WT mice (Supplemental Fig. 1A). Furthermore, the expression levels of other cytokines, such as *Il12a*, *Il22*, and *Il4*, which are associated with the maintenance of barrier integrity, were not significantly altered in *Irf7*$^{-/-}$ mice in comparison to WT mice (Supplemental Fig. 1B–D).

The intestinal epithelial barrier, which separates the intestinal lumen and the mucosa, plays a crucial role in protecting the host against microbial infections. The intestinal barrier is comprised of a single, intact layer of intestinal epithelial cells (IECs) and their secreted mucus proteins, as well as tight junction (TJ) proteins such as E-cadherin, β-catenin, Occludin, and ZO-1, desmosomes, and anti-microbial peptides [32]. Previous studies have demonstrated that Occludin and Claudin-5 play a role in regulating intestinal epithelial integrity [33, 34]. To investigate which genes associated with the intestinal barrier are defective in *Irf7*$^{-/-}$ mice during colitis development, we analyzed the gene expression of mucus-related genes (including *Muc1*, *Muc2*, *Muc3*, and *Muc4*), tight junction-related genes (including *Cdh1(E-cadherin)*, *Ctnnb1(β-catenin)*, *Cldn1(Claudin1)*, *Cldn2(Claudin2)*, *Cldn3(Claudin3)*, *Cldn4(Claudin4)*, *Cldn5(Claudin-5)*, *Cldn11(Claudin11)*, *Ocln(Occludin)*, *Tjp1(Zo1)*, and *Desmocollin1*, *Desmocollin2*, *Desmocollin3*, *Desmoplakin*), and other related genes (including *Vim(Vimentin)*, *Tff3*, *S100a8*, *S100a9*, *Reg3β*, *Reg3γ* and *Lcn2*). The findings indicate that the gene expression of *Muc2*, *Cdh1*, *Ctnnb1*, and *Ocln* was significantly decreased in the colon tissues of *Irf7*$^{-/-}$ mice compared to WT mice, while the expression levels of other genes

(See figure on next page.)

Fig. 3 The alteration in expression level of genes associated with intestinal epithelial integrity in *Irf7*$^{-/-}$ mice after DSS treatment. Six mice, including 3 WT and 3 *Irf7*$^{-/-}$ mice, were subjected to a treatment regimen consisting of 3% DSS for five days followed by regular water for 3 days. The other 6 mice (including 3 WT mice and 3 *Irf7*$^{-/-}$ mice) were treated with regular water without DSS. On day 8, all mice were administered FITC-Dextran via gavage, and serum samples were collected 3 h later for the detection of FITC-dextran (**A**). The expression levels of colonic mucus-related genes, namely *Muc1*, *Muc2*, *Muc3*, and *Muc4*, were determined using RT-qPCR (**B**–**E**). Additionally, the expression levels of epithelial cell junction-related genes, including *Cdh1 (E-cadherin)*, *Ctnnb1 (β-catenin)*, *Cldn1 (Claudin1)*, *Cldn2 (Claudin2)*, *Cldn3 (Claudin3)*, *Cldn4 (Claudin4)*, *Cldn5 (Claudin-5)*, *Cldn11 (Claudin11)*, *Ocln (Occludin)*, *Tjp1 (Zo-1)*, *Desmoplakin*, *Desmocollin1*, *Desmocollin2*, and *Desmocollin3* were also assessed via RT-qPCR (**F**–**S**). In (**B**–**S**), D0: WT (n = 4), *Irf7*$^{-/-}$ (n = 4), D8: WT (n = 5), *Irf7*$^{-/-}$ (n = 5). The experiment was independently repeated two times. In **(A-S)**, the data are expressed as mean ± s.e.m. NS, not significant, *$P < 0.05$, **$P < 0.01$, ***$P < 0.001$. Unpaired two-tailed student's *t*-test (**A**), Two-way ANOVA with Holm-Sidak's multiple comparisons test (**B**-**S**)

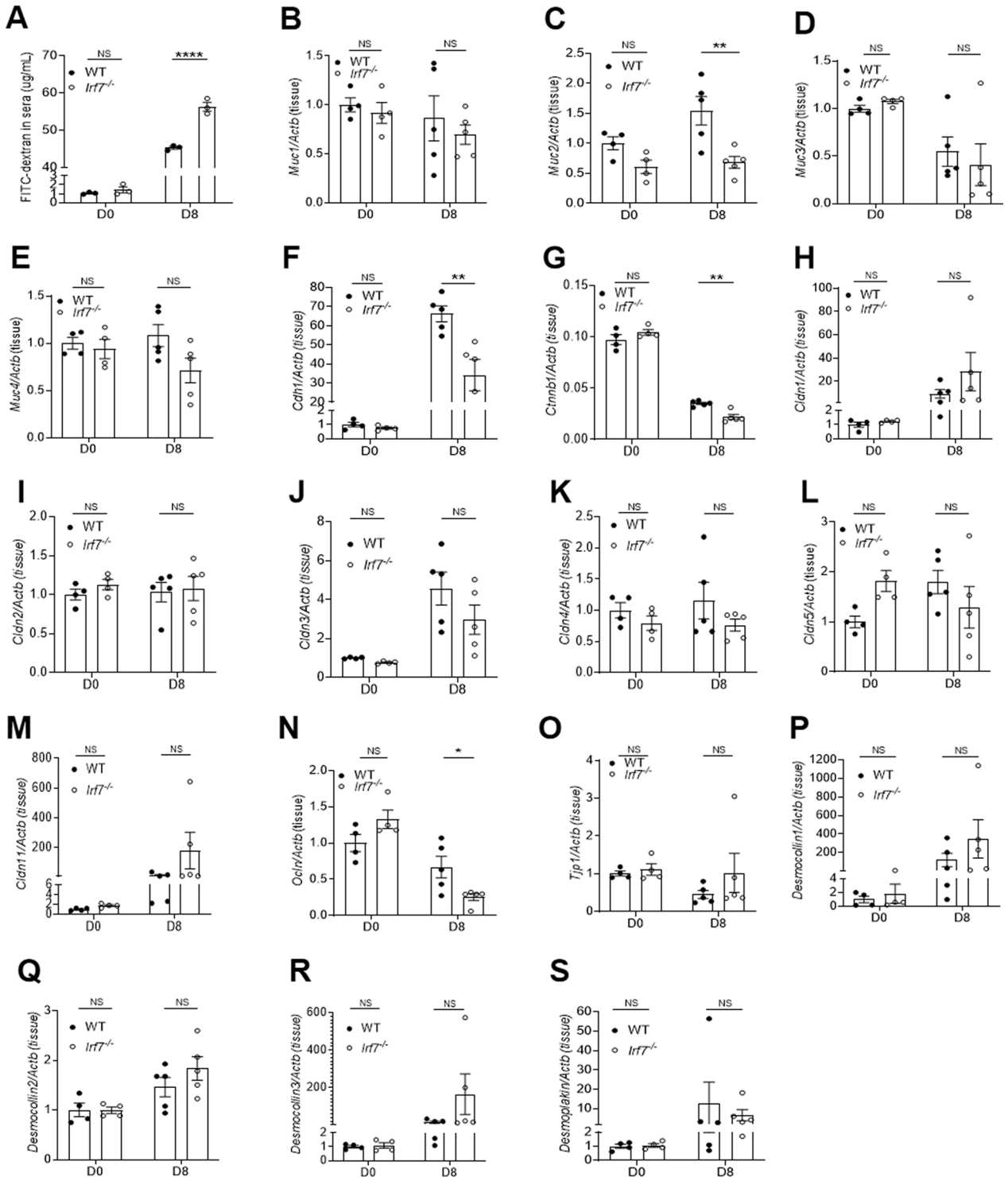

Fig. 3 (See legend on previous page.)

remained unaltered due to IRF7 deficiency (Fig. 3B–S, Supplemental Fig. 2A–G).

Additionally, the protein expressions of Muc2, E-cadherin, β-catenin, and Occludin were measured in colonic tissues of mice on day 0 and 8 after DSS treatment using Western-blot and immunofluorescence assay. The results revealed a marked reduction in Muc2, E-cadherin, β-catenin, and Occludin in *Irf7*$^{-/-}$ mice in comparison to

WT mice (Fig. 4A–F). The PAS staining analysis revealed that *Irf7*$^{-/-}$ mice exhibited compromised intestinal epithelial barrier integrity and less mucus secretion from goblet cells in comparison to WT mice (Fig. 4G). These findings suggest that the suppression of Muc2, E-cadherin, β-catenin, and Occludin in *Irf7*$^{-/-}$ mice may result in the disruption of the epithelial barrier, leading to bacterial invasion and ultimately triggering the release of inflammatory cytokines or related molecules, thereby increasing susceptibility to colitis.

The enhanced susceptibility of DSS-induced colitis in *Irf7*$^{-/-}$ mice is associated with the defect in the production of IFN-III, but not IFN-I or IFN-II

We then aim to elucidate the underlying mechanism by which IRF7 regulates Muc2, E-cadherin, β-catenin, and Occludin to enhance epithelial integrity. During the advanced stages of infection, the translocation of activated IRF7 to the nucleus results in the induction of interferon production [35]. Type I interferons, namely IFN-α and IFN-β, exhibit diverse biological activities and play a crucial role in maintaining immune homeostasis following intestinal epithelial injury [36]. Consequently, we evaluated the gene and protein expression levels of IFN-α and IFN-β in the colonic tissues and sera of both WT and *Irf7*$^{-/-}$ mice. However, no significant difference in the levels of IFN-α and IFN-β was observed in the sera and colonic tissues of *Irf7*$^{-/-}$ and WT mice (Fig. 5A–F). The expression of Type II interferons, specifically IFN-γ, did not exhibit any significant changes between the experimental and control groups (Fig. 5G–I). These findings suggest that the augmented susceptibility of *Irf7*$^{-/-}$ mice to DSS-induced colitis may not be linked to IFN-I or IFN-II production.

As previously mentioned, IRF7 plays a role in regulating the production of IFN-III (IL-29, IL-28A, and IL-28B), which are implicated in intestinal integrity and inflammatory responses [37, 38]. However, the extent to which IRF7 regulates IFN-III in the development of colitis remains unclear. In light of the absence of IL-29 expression in mice, we conducted an investigation into the gene and protein levels of IL-28A and IL-28B in the colonic tissues of both WT and *Irf7*$^{-/-}$ mice during the progression of colitis. Our findings revealed that *Irf7*$^{-/-}$ mice exhibited significantly lower levels of IL-28A at both the gene and protein levels in comparison to WT mice. However, there was no significant alteration in the expression of IL-28B between the two groups (Fig. 5J–M). In addition, there were no significant gene expression differences in IL-28RA and IL-10RB, the heterodimeric receptor complexes for IL-28A (Supplementary Fig. 2H, I). This suggests that *Irf7* may mediate IL-28A production but does not affect IL-28A receptor expression. The above results suggest that the heightened susceptibility of *Irf7*$^{-/-}$ mice to colitis is not reliant on IFN-I and may instead be attributed to the deficiency in IFN-III production.

It is noteworthy that macrophages were the primary source of IFN-III [39]. To further investigate the potential direct regulation of IFN-III expression in macrophages by IRF7, we cultured BMDM from both WT and *Irf7*$^{-/-}$ mice and stimulated them with poly(I:C). The secreted IL-28A of BMDM was subsequently examined at 0 and 24 h after poly(I:C) treatment. Our findings indicate that the secreted IL-28A, but not IL-28B, in BMDM from *Irf7*$^{-/-}$ mice was significantly attenuated at 24 h after stimulation compared to BMDM from WT mice (Fig. 5N, O). Furthermore, we observed a noticeable inhibition of IFN-α and IFN-β gene and protein expression in BMDM from *Irf7*$^{-/-}$ mice compared to BMDM from WT mice after Poly(I:C) stimulation (Supplemental Fig. 3A–D). The findings obtained from in vitro experiments were consistent with prior literature [40], however, they were incongruent with our in vivo results as depicted in Fig. 5. This discrepancy may be attributed to the dissimilar composition of BMDM and colon tissues.

Additionally, the levels of gene expression of pro-inflammatory cytokines, such as *Il6*, *Tnf*, *Il1b*, *KC*, and *MCP-1*, did not exhibit any significant difference between *Irf7*$^{-/-}$ mice and WT mice. This could be due to the fact that BMDM, which were stimulated by poly(I:C), did not have a significant impact on the pro-inflammatory cytokine production pathway (Supplemental Fig. 4A–E).

To investigate whether IRF7 promotes IL-28A expression in other cell types, such as intestinal epithelial cells, we transfected the pcDNA3.1-IRF7 plasmid into the human epithelial cell line, HCT116, for 24 h prior to Poly(I:C) stimulation to assess the expression of IRF7,

(See figure on next page.)

Fig. 4 The protein expression of molecules associated with epithelial barrier in *Irf7*$^{-/-}$ mice after DSS treatment. WT and *Irf7*$^{-/-}$ mice were administered 3% DSS, and subsequently, sera and colons were collected on days 0 and 8. Colonic samples were collected, extracted and tested for protein levels of Muc2, E-cadherin, β-catenin and Occludin by Western-blot (**A**–**E**) and Immunofluorescence analysis (**F**). Detection of goblet cells by PAS staining (**G**). Scale bar, 50 μm. D0: WT (n = 4), *Irf7*$^{-/-}$ (n = 4), D8: WT (n = 5), *Irf7*$^{-/-}$ (n = 5). The experiment was independently repeated two times. The data are expressed as mean ± s.e.m. NS, not significant, $^{**}P < 0.01$, $^{***}P < 0.001$, $^{****}P < 0.0001$. Two-way ANOVA with Holm-Sidak's multiple comparisons test (**B**–**E**)

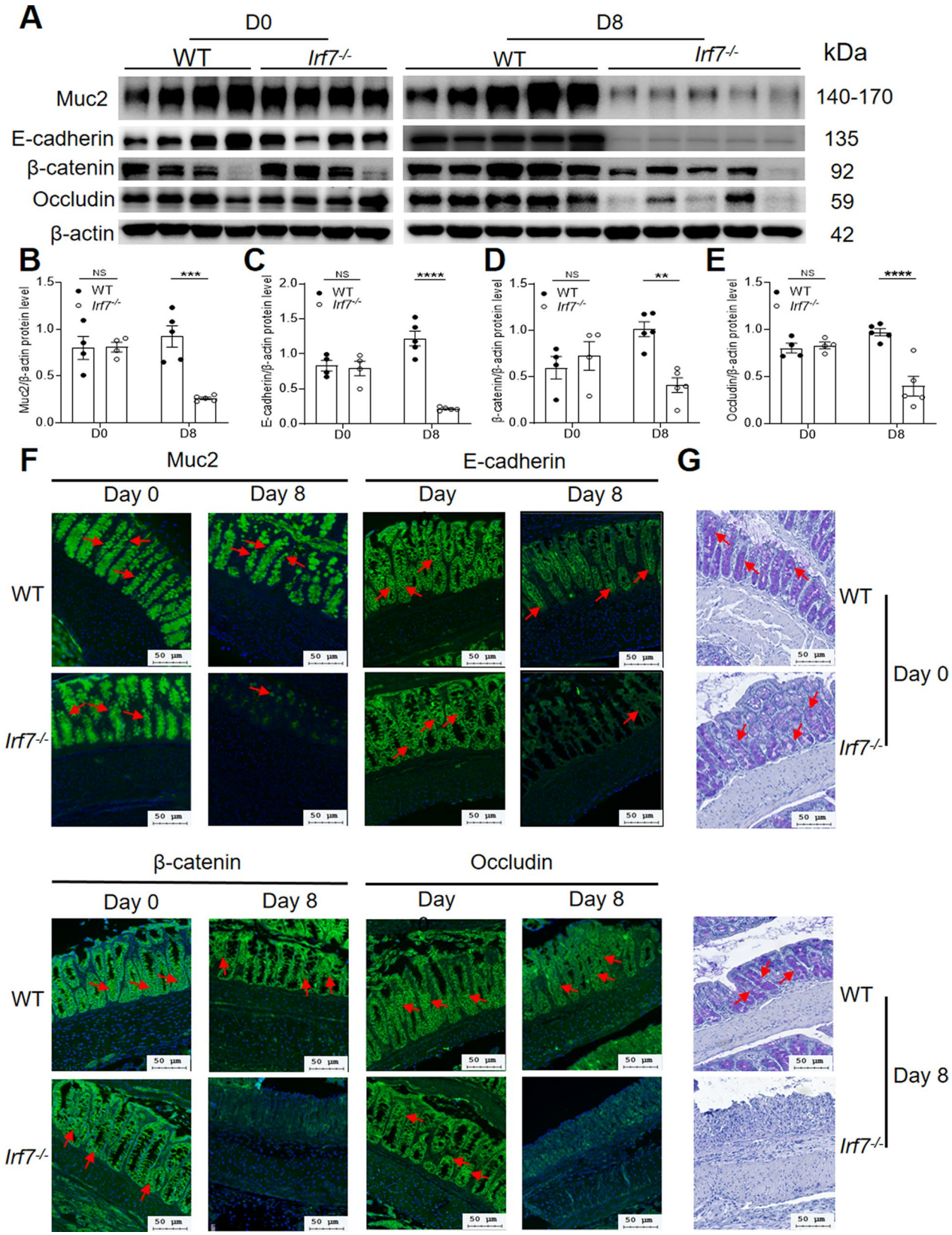

Fig. 4 (See legend on previous page.)

IL28RA, IL28A, and IL28B. The overexpression of IRF7 was confirmed using RT-qPCR (Supplemental Fig. 5A). The results revealed that HCT116 cells exhibited expression of IL28 receptor, and upon poly(I:C) stimulation, cells transfected with pcDNA3.1-IRF7 plasmid demonstrated significantly lower levels of IL28A expression in comparison to the control group, while IL28B expression remained unchanged (Supplemental Fig. 5B-C). These findings suggest that IRF7 may primarily induce IL-28A expression in macrophages. However, this conclusion needs to be further verified using tools such as *Irf7*$^{fl/fl}$-*Lyzcre* mice.

IL-28A treatment enhances the expression of molecules associated with barrier function in intestinal epithelial cells

As previously mentioned, IL-28A plays a crucial role in regulating intestinal epithelial barrier function. To confirm this, we first backfilled HCT116 cells with recombinant IL-28A and detected the expression of intestinal epithelial barrier-related genes by RT-qPCR to determine the role of IL-28A on the intestinal epithelial barrier. Our findings indicate a significant up-regulation in the expression of MUC2, CDH1, CTNNB1, and OCLN following the administration of IL-28A. Conversely, no notable differences were observed in the expression of other genes (Supplementary Fig. 6A-R). To further confirm this, we again stimulated intestinal epithelial cells, including HCT116 and Caco2 cells, with recombinant IL-28A, and detected the levels of intestinal epithelial barrier-associated proteins by Western-blot to further substantiate its function. The Western-blot analysis revealed that the stimulation of IL-28A significantly upregulated the expression of Muc2, E-cadherin, β-catenin, and Occludin in both HCT116 (Supplemental Fig. 7A-E) and Caco2 cells (Supplemental Fig. 7F–J), suggesting a direct enhancement of the molecules associated with intestinal epithelial cell barrier functions. These results suggest that IL-28A exerts regulatory control over Muc2, E-cadherin, β-catenin, and Occludin at both the protein and gene levels.

Amelioration of the high susceptibility of *Irf7*$^{-/-}$ mice to DSS-induced colitis by IL-28A supplement

To validate the in vivo functionality of IL-28A, we administered IL-28A recombinant protein to DSS-treated *Irf7*$^{-/-}$ mice via intraperitoneal injection on day 5 after DSS treatment. We confirm successful establishment of IL-28A recombinant protein injection in *Irf7*$^{-/-}$ mice, as evidenced by significantly increased serum levels of IL-28A in comparison to PBS-injected mice (Fig. 6A). Moreover, there was no significant gene expression difference in IL-28RA and IL-10RB. This suggests that injection of IL-28A recombinant protein does not affect the expression of IL-28A receptors (Supplemental Fig. 8A–B). Subsequent observation revealed a decrease in body weight of DSS-fed mice, with *Irf7*$^{-/-}$ mice exhibiting more severe weight loss on days 5–8 post-treatment than their IL-28A-injected counterparts (Fig. 6B). Consistently, following DSS treatment, *Irf7*$^{-/-}$ mice administered with IL-28A recombinant protein exhibited heightened resistance against colitis, as evidenced by improvements in fecal viscosity, rectal bleeding scores, and increased colon length (Fig. 6C–F). Additionally, histological analysis via H&E staining revealed a reversal of the previously observed tissue damage following IL-28A treatment (Fig. 6G). These findings suggest that the supplementation of IL-28A may effectively ameliorate the heightened susceptibility of *Irf7*$^{-/-}$ mice to DSS-induced colitis.

Supplement of IL-28A attenuates the intestinal epithelial permeability and suppresses the expression of intestinal barrier-associated molecules in *Irf7*$^{-/-}$ mice during colitis development.

To determine whether IL-28A mediates the protective effect of IRF7 in preserving intestinal epithelial integrity and shielding mice from DSS-induced colitis, we conducted an investigation into the intestinal epithelial permeability of mice that received IL-28A injections. Our findings indicate that the serum concentration of FITC-dextran was significantly reduced in *Irf7*$^{-/-}$ mice that received IL-28A injections, as compared to those that did not receive IL-28A injections (Fig. 6H). This suggests that

(See figure on next page.)

Fig. 5 The enhanced susceptibility of DSS-induced colitis in *Irf7*$^{-/-}$ mice is associated with the defect in the production of IFN-III, but not IFN-I or IFN-II. WT and *Irf7*$^{-/-}$ mice were administered 3% DSS, and subsequently, sera and colons were collected on days 0 and 8. The expression levels of *Ifna* and *Ifnb1* genes in colon tissues were detected by RT-qPCR (**A**, **B**). The levels of IFN-α and IFN-β proteins in colon tissues and sera were measured by ELISA (**C**–**F**). The expression levels of *Ifng* gene in colon tissues were detected by RT-qPCR (**G**). The levels of IFN-γ protein in colon tissues and sera were measured by ELISA (**H**, **I**). The expression levels of *Il28a* and *Il28b* genes in colon tissues were detected by RT-qPCR (**J**, **K**). The levels of *Il28a* and *Il28b* proteins in colon tissues were measured by ELISA (**L**–**M**). D0: WT (n = 4), *Irf7*$^{-/-}$ (n = 4), D8: WT (n = 5), *Irf7*$^{-/-}$ (n = 5) of RT-qPCR. D0: WT (n = 3), *Irf7*$^{-/-}$ (n = 3), D8: WT (n = 5), *Irf7*$^{-/-}$ (n = 5) of ELISA. BMDM of WT and *Irf7*$^{-/-}$ mice were stimulated with 1 μg Poly(I:C) for 0 h and 24 h, and then supernatants were collected to detect IL-28A and IL-28B protein levels using ELISA (**N**–**O**). WT and *Irf7*$^{-/-}$ BMDM at each time point, n = 3 at each time point in both groups. The experiment was independently repeated two times. The data are expressed as mean ± s.e.m. NS, not significant, **P* < 0.05, ***P* < 0.01. Two-way ANOVA with Holm-Sidak's multiple comparisons test (**A**–**O**)

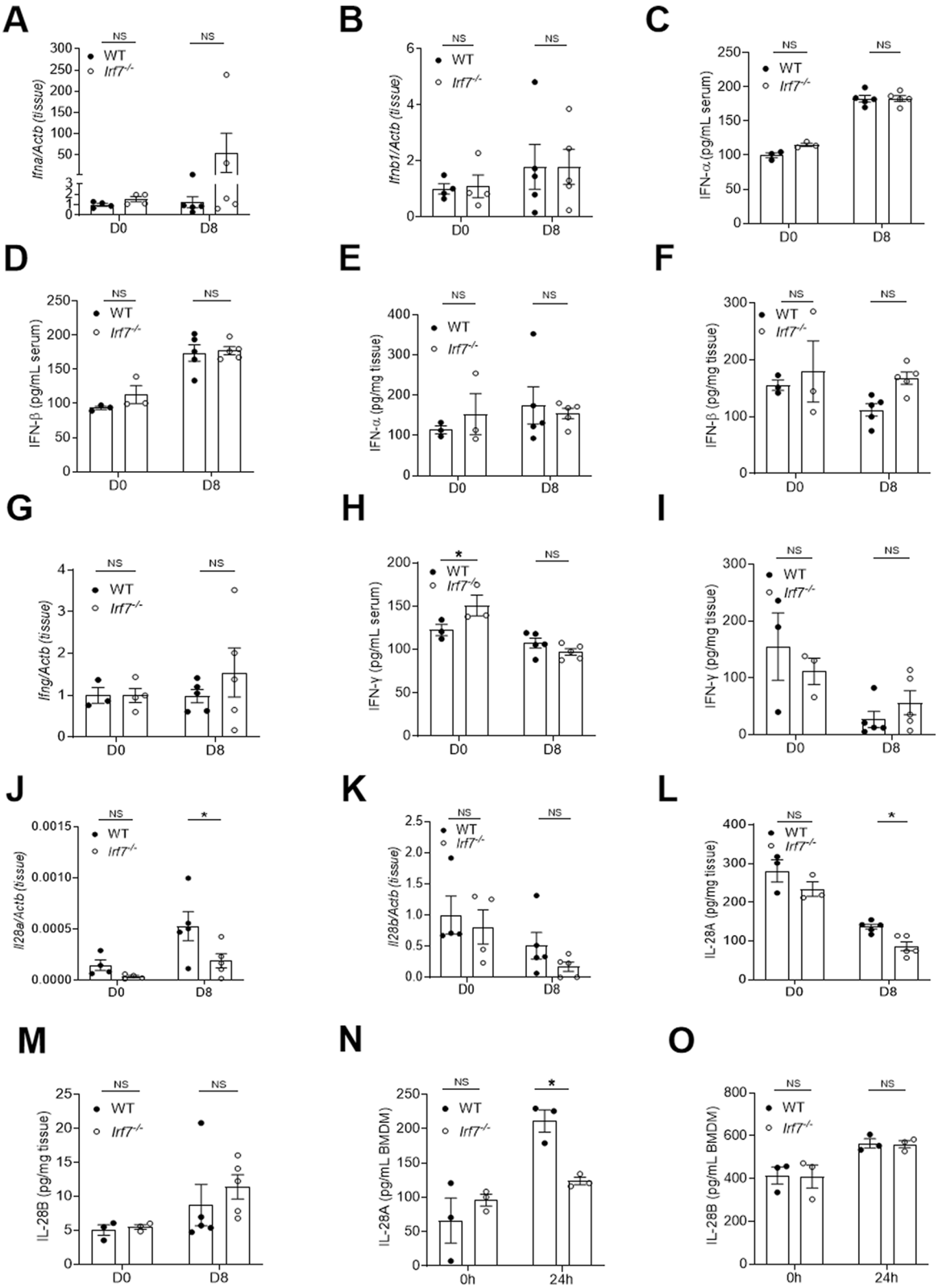

Fig. 5 (See legend on previous page.)

the administration of IL-28A mitigated the intestinal epithelial permeability caused by DSS treatment. Moreover, the administration of IL-28A supplement resulted in a significant upregulation of Muc2, E-cadherin, β-catenin, and Occludin expression levels in the colonic tissues of *Irf7*$^{-/-}$ mice following DSS treatment (Fig. 6I-M). This reduction in epithelial permeability could potentially impede bacterial invasion, immune cell activation, and inflammatory cytokine secretion in the intestine. It is noteworthy that the IL-28A recombinant protein-mediated enhancement of intestinal epithelial barrier-related molecules was consistent both in vitro and in vivo, thus underscoring the pivotal role of IL-28A in maintaining the integrity of the intestinal epithelial barrier. Overall, IRF7 may stimulate the production of IL-28A, which in turn upregulates the expression of Muc2, E-cadherin, β-catenin, and Occludin, thereby promoting the integrity of the epithelial barrier and mitigating intestinal inflammation (Supplemental Fig. 9).

Discussion

The incidence of IBD has been on the rise in developing countries [41], and its pathogenesis is linked to genetic anomalies, immune dysregulation, gut microbiota, and environmental factors [42–44]. Therefore, it is crucial to investigate the underlying mechanisms of IBD to facilitate the development of targeted therapeutic interventions. The interplay between the immune system and intestinal microbiota plays a crucial role in the development of IBD. In both normal and abnormal physiological states, pathogen-associated molecular patterns (PAMPs) of bacterial and viral origin, such as lipopolysaccharides, proteins, and nucleic acids, are detected by PRRs. This triggers the activation of downstream signaling pathways, including the NF-κB and IFN pathways, leading to the production of inflammatory cytokines and IFNs, ultimately resulting in intestinal inflammation [45].

Results from both human disease databases and clinical patients suggest that IRF7 expression is significantly reduced in UC patients. Similarly, our experimental findings indicate that *Irf7*$^{-/-}$ mice exhibit a heightened susceptibility to DSS-induced colitis, as evidenced by a range of phenotypic markers such as increased mortality, weight loss, fecal viscosity, and rectal bleeding scores. These results suggest that IRF7 plays a crucial role in host resistance to DSS-induced colitis, potentially by modulating the microenvironment and suppressing inflammation. Previous studies have shown that IRF7 can induce abnormal IFN-I expression, leading to enhanced inflammation in conditions such as systemic sclerosis and autoimmune pancreatitis [22, 46]. Additionally, IRF7 produced by BMDM in a cholesterol-rich environment may contribute to the development of atherogenesis [21]. In the context of adipose inflammation associated with obesity, the expression of MCP-1, an adipokine, is induced by IRF7, leading to inflammation [23]. Another study found that IRF7 upregulates SLC11A2 transcription by inhibiting miR-375-3p expression, which promotes iron death and UC progression in colonic epithelial cells of DSS-treated mice [47]. However, our findings demonstrate that IRF7 inhibits the progression of DSS-induced colitis. This may be attributed to the different system for Irf7 (Injection of overexpression vector versus knockout mice), which reinforces the fact that the role of IRF7 is complex and controversial, and needs to be further explored.

Notably, IRF7 functions as a transcription factor that facilitates the production of IFN-I during viral infections. It is noteworthy that the viral infection of mice with WT, *Irf3*$^{-/-}$*Irf7*$^{-/-}$, *Irf3*$^{-/-}$, and *Irf7*$^{-/-}$ genotypes did not exhibit any significant differences in viral load in the airway epithelial cells and lung tissue of *Irf3*$^{-/-}$ and *Irf7*$^{-/-}$ mice when compared to WT mice. However, the viral load in the airway epithelial cells and lung tissue of *Irf3*$^{-/-}$*Irf7*$^{-/-}$ mice was significantly higher [48]. The detection of IFN-α revealed that the levels of IFN-α were not significantly reduced in either *Irf3*$^{-/-}$ or *Irf7*$^{-/-}$ mice when compared to WT mice. In contrast, the levels of IFN-α were significantly reduced in *Irf3*$^{-/-}$*Irf7*$^{-/-}$ mice [48]. This demonstrates that in certain instances, the effective production of IFN-α necessitates the collaborative function of both IRF3 and IRF7, and the absence of one transcription factor alone may not result in a substantial reduction in IFN-I. Additionally, the removal of

(See figure on next page.)

Fig. 6 Supplementation of IL-28A recombinant protein reduces the susceptibility of *Irf7*$^{-/-}$ mice to DSS-induced colitis by maintaining intestinal epithelial barrier function. WT and *Irf7*$^{-/-}$ mice were administered 3% DSS, and then injected intraperitoneally with IL-28A recombinant protein (2 μg/mice) on day 5. Mice were sacrificed on day 8 and sera were collected for measuring the IL-28A protein expression (**A**). **B** Body weight change, **C** stool consistency scores; **D** bleeding scores, **E** colon length, **F** representative images of colon, **G** H & E staining of colon on day 8. Scale bar, 100 μm. FITC-dextran was gavaged on day 8 and sera was collected 3 h later to detect FITC-Dextran concentration **(H)**. Colons were collected to detect the protein expression levels using Western-blot. **I, J** Muc2, **I**, **K** E-cadherin, **I**, **L** β-catenin, **I**, **M** Occludin protein expression were shown. WT + DSS + PBS (n = 4), *Irf7*$^{-/-}$ + DSS + PBS (n = 5), *Irf7*$^{-/-}$ + DSS + IL-28A (n = 5). The experiment was independently repeated two times. In **A**-**E**, **H** and **J**-**M**, the data are expressed as mean ± s.e.m. NS, not significant, *$P < 0.05$, **$P < 0.01$, ***$P < 0.001$, ****$P < 0.0001$. One-way ANOVA with Dunnett's multiple comparisons test (**A**, **E**, **H**, **J**-**M**) and Two-way ANOVA with Holm-Sidak's multiple comparisons test **B**-**D**

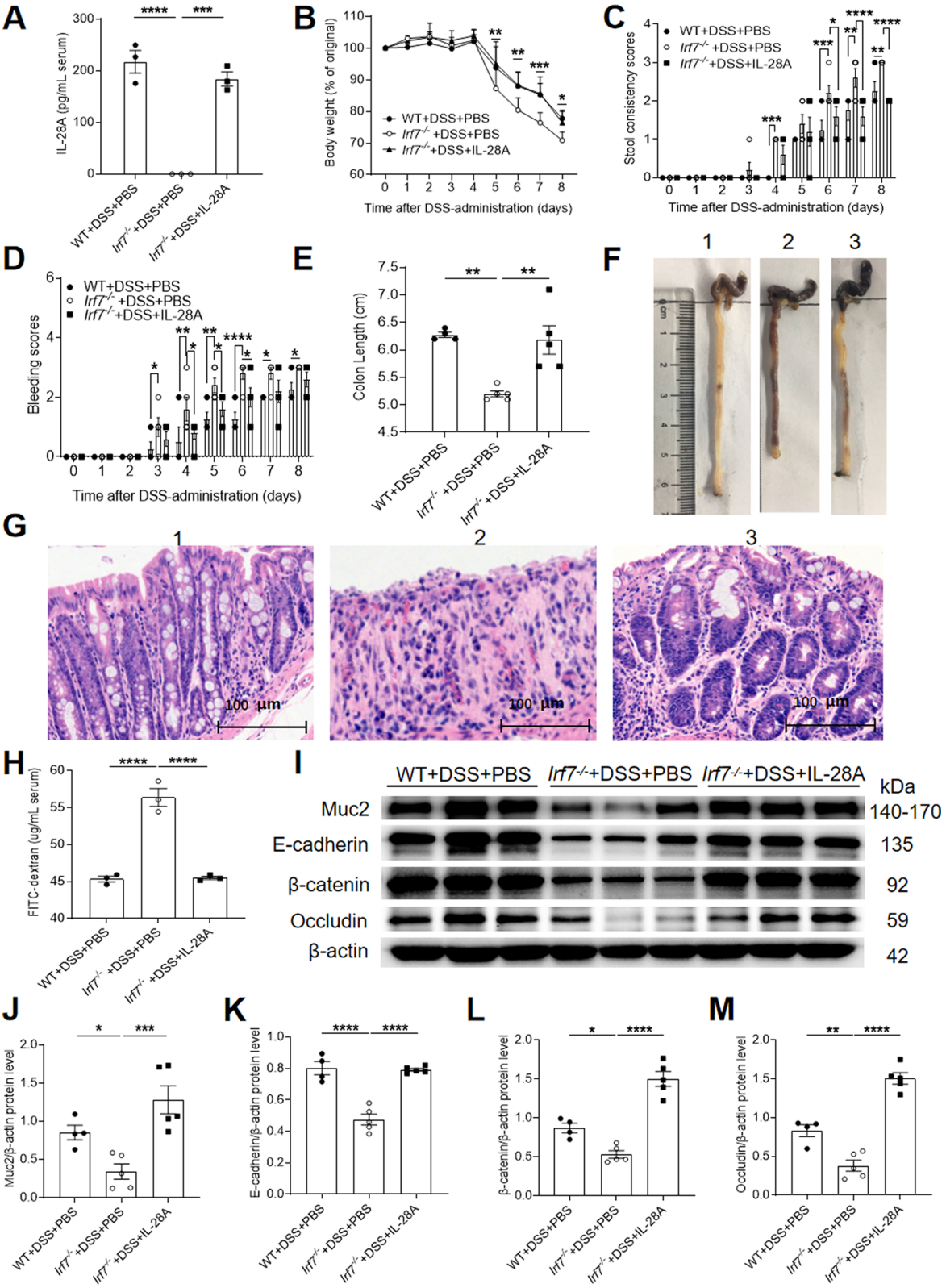

Fig. 6 (See legend on previous page.)

IRF7 in epithelial cells did not significantly impact IFN-α production during viral infection [48]. Moreover, the induction of IFN-β production in bone marrow-derived dendritic cells (BMDC) from both WT and *Irf7*$^{-/-}$ mice through LPS or fungal Curdlan stimulation did not exhibit any noteworthy differences, indicating that IRF7 does not play a role in IFN-β production by BMDC during fungal infection [49, 50]. This suggests that, in specific circumstances such as varying cell types or infections, the production of IFN-I may not rely solely on the transcription factor IRF7.

Our findings demonstrate that *Irf7*$^{-/-}$ mice did not exhibit a significant reduction in IFN-α and IFN-β production in colonic tissues during DSS-induced colitis when compared to control mice. This disparity may be attributed to the intricate cell types present in colonic tissues or diverse environmental stimuli, such as gut microbiota, or the dependence on both IRF7 and IRF3. In our experiment, it was observed that BMDM from *Irf7*$^{-/-}$ mice exhibited a significant reduction in IFN-I production as compared to WT mice when subjected to Poly(I:C) stimulation. This finding suggests that the deletion of IRF7 has an impact on IFN-I production in macrophages under specific ligand stimulation, which is consistent with prior literature [50, 51]. Consequently, we postulate that the IRF7-IFN-I pathway may not be the primary mechanism through which IRF7 confers host resistance to DSS-induced colitis.

DSS treatment can disrupt the intestinal epithelium, leading to the loss of crypt structure and mucosal ulceration, which led to increased intestinal epithelial permeability. The present study suggests that IRF7-mediated IL-28A production in colonic tissues plays a crucial role in safeguarding the integrity of the intestinal barrier. Specifically, IRF7 was found to enhance the expression of Muc2, E-cadherin, β-catenin, and Occludin, thereby promoting the protection of the intestinal epithelial barrier in colonic tissue. This may be different from the previously reported tight junction of the intestine in UC [52]. The intestinal barrier is composed of a singular, intact layer of intestinal epithelial cells (IECs) and their secreted mucus proteins, along with tight junction (TJ) proteins such as E-cadherin, β-catenin, Occludin, and ZO-1, desmosomes, and anti-microbial peptides. Yu M et al. study exhibited decreased levels of ZO-1, Occludin, and Claudin-1 in DSS-induced colitis, consequently leading to impaired functionality of the intestinal epithelial barrier [53]. In a study conducted by Li X et al. [54] on DSS-induced colitis, it was observed that the levels of ZO-1 and Occludin were reduced, leading to an increase in permeability of the intestinal epithelial barrier. Similarly, Samak G et al. [55] discovered that DSS treatment resulted in the disruption of the intestinal epithelial barrier through the downregulation of E-cadherin, β-catenin, Occludin, and ZO-1. Additionally, Zhang Z et al. [56] found that eicosapentaenoic acid (EPA) administration could effectively upregulate Claudin-1 and Occludin, thereby mitigating the development of DSS-induced colitis. Hence, it is our opinion that the factors responsible for the disruption of the intestinal epithelial barrier are not single, and the markers indicating barrier damage are not universally constant, mirroring the intricate pathogenesis of UC and the potential variability in molecular mechanisms. Consequently, tight junction proteins may undergo alterations due to diverse upstream signaling regulations, ultimately impacting the integrity of the intestinal epithelial barrier. Notably, IFN-III is primarily involved in intestinal mucosal immunity [57], and previous research has demonstrated that IRF7 can limit the invasion of *Salmonella* and prevent damage to human epithelial cells during *Salmonella* infection [37]. Additionally, IRF7 has been shown to upregulate the expression of Claudin-5 in endothelial cells and airway epithelial cells [33]. Furthermore, IL-28A has been demonstrated to exhibit anti-inflammatory properties, thereby inhibiting collagen-induced arthritis through the suppression of IL-1β expression (58). Additionally, IL-28A has been shown to regulate lung dendritic cells, thereby suppressing airway allergic inflammation [59].

Currently, there is controversy regarding the role of IL-28A on the intestinal epithelial barrier. A previous investigation conducted by Xu P et al. demonstrated that the introduction of IL-28A (500 ng/mL for 24 h) to intestinal organoids derived from CD patients could disrupt the epithelial barrier. Additionally, the study revealed that elevated concentrations of IL-28A (1000 ng/mL) yielded similar outcomes in Caco2 cells, whereas low concentrations of IL-28A did not achieve disruption of the intestinal epithelial barrier [60]. In an intestinal ischemia/reperfusion (I/R) model, Li L et al. observed a reduction in Claudin-1, Occludin, and ZO-1 expression, as well as increased permeability, in the model group compared to the control group. However, these effects were reversed upon administration of recombinant IL-28A. Similar findings were obtained through simultaneous incubation of Caco2 cells with IL-28A (100 nM for 12 h), indicating that IL-28A can effectively preserve the integrity of the intestinal epithelial barrier [32]. These results suggest that the functional role of IL-28A may vary depending on its concentration. The results of our study indicate that in DSS-induced colitis, the levels of Muc2, E-cadherin, Occludin, and β-catenin were significantly reduced in *Irf7*$^{-/-}$ mice. However, when these mice were treated with IL-28A recombinant protein, there was a significant increase in the levels of these proteins, leading to a reversal of the susceptibility to DSS-induced colitis. These

findings suggest that IL-28A may play a role in maintaining the integrity of the intestinal epithelial barrier by upregulating Muc2, E-cadherin, Occludin, and β-catenin. Additionally, consistent results were obtained through in vitro culturing of HCT116 and Caco2 cells following the administration of IL-28A recombinant proteins at doses of 100 ng/mL and 300 ng/mL, respectively. UC and CD exhibit disparities concerning the site of onset, breadth and depth of lesions, clinical manifestations, and therapeutic strategies, and they may also exert diverse effects through their regulatory mechanisms. Consequently, while IL-28A has been demonstrated to impair the integrity of the intestinal epithelial barrier in CD patients, it seems that varying concentrations of IL-28A might also contribute to the preservation of the intestinal epithelial barrier in UC patients.

Further investigation is necessary to explore the findings presented herein, which indicate that IL-28A may stimulate the expression of Muc2, E-cadherin, β-catenin, and Occludin. Muc2 is secreted by goblet cells, while E-cadherin, β-catenin, and Occludin are expressed in epithelial cells. IL-28A is involved in the development of colitis and a more comprehensive analysis is required to elucidate the mechanisms by which macrophage IL-28A regulates the expression of Muc2 in goblet cells and E-cadherin, β-catenin, and Occludin in epithelial cells. As mentioned above, IL-28A upregulates Claudin-1 expression and maintains intestinal epithelial barrier function through the p-STAT1 pathway [32]. Therefore, we hypothesized that IRF7 can promote IL-28A expression, which promotes STAT1 phosphorylation through downstream signaling pathways, such as the JAK-STAT pathway, which in turn regulates TJ proteins such as β-catenin and ultimately protects the intestinal epithelial barrier. Nonetheless, an examination of the activation of pathways in *Irf7*$^{-/-}$ mice during DSS-induced colitis has yet to be conducted.

To summarize, this investigation has established the involvement of IRF7 in the regulation of IL-28A expression, thereby safeguarding the integrity of the epithelial barrier and diminishing the host's vulnerability to colitis development. The innovative roles of IRF7 may present a fresh immune target for the management of IBD.

Supplementary Information

The online version contains supplementary material available at https://doi.org/10.1186/s12967-024-05673-y.

Supplementary file 1.

Supplementary file 2: Supplemental Figure 1. The effect of *Irf7* deficiency on some cytokine expression during colitis development. WT and *Irf7*$^{-/-}$ mice were administered 3% DSS and colons were collected on days 0 and 8 after DSS treatment, respectively, for detecting the cytokine expression levels by ELISA or RT-qPCR assays. (A) IL-33 protein expression. (B) Il12a, (C) Il22, (D) Il4. D0: WT (n=4), *Irf7*$^{-/-}$ (n=4) and D8: WT (n=5), *Irf7*$^{-/-}$ (n=5). The data are expressed as mean ± s.e.m. NS, not significant. Two-way ANOVA with Holm-Sidak's multiple comparisons test (A-F). Supplemental Figure 2. The alteration in expression level of genes associated with intestinal epithelial integrity and IL-28A receptor in *Irf7*$^{-/-}$ mice after DSS treatment. WT and *Irf7*$^{-/-}$ mice were administered 3% DSS and colons were collected on days 0 and 8 after DSS treatment. (A) *Tff3*, (B) *Vim (Vimentin)*, (C) *S100a8*, (D) *S100a9*, (E) *Reg3β*, (F) *Reg3γ*, (G) *Lcn2*, (H) *Il10rb* and (I) *Ifnlr1* were detected by RT-qPCR. D0: WT (n=4), *Irf7*$^{-/-}$ (n=4), D8: WT (n=5), *Irf7*$^{-/-}$ (n=5). In (A-I), the data are expressed as mean ± s.e.m. NS, not significant. Two-way ANOVA with Holm-Sidak's multiple comparisons test (A-I). Supplemental Figure 3. *Irf7*$^{-/-}$mouse BMDM are defective in IFN-α and IFN-β expression under poly(I:C) stimulation. WT and *Irf7*$^{-/-}$ mouse BMDM were stimulated with 1 μg of poly(I:C). Cells were collected at 0, 1, 2 and 4 hours after stimulation, and (A) *Ifna* and (B) *Ifnb1* gene expression were detected using RT-qPCR. Cell supernatants were collected at 0, 8, and 24 h and (C) IFN-α and (D) IFN-β protein levels were measured using ELISA.WT and *Irf7*$^{-/-}$ BMDM at each time point, n=3. The data are expressed as mean ± s.e.m. NS, not significant, *P < 0.05, **P < 0.01, ***P < 0.001, ****P < 0.0001. Two-way ANOVA with Holm-Sidak's multiple comparisons test (A-D). Supplemental Figure 4. *Irf7*$^{-/-}$ and WT mouse derived BMDM have similar levels of inflammatory cytokines expression under poly(I:C) stimulation. WT and *Irf7*$^{-/-}$ mouse BMDM were stimulated with 1 μg of poly(I:C). Cells were collected at 0, 1, 2, and 4 hours after stimulation and (A) *Il6*, (B) *Tnf*, (C) *Il1b*, (D) *KC*, and (E) *MCP-1* gene expression were detected using RT-qPCR. WT and *Irf7*$^{-/-}$ BMDM at each time point, n=3. The data are expressed as mean ± s.e.m. NS, not significant. Two-way ANOVA with Holm-Sidak's multiple comparisons test (A-E). Supplemental Figure 5. The effect of IRF7 on IL-28A production in intestinal epithelial cells. HCT116 cells were transfected with 1 μg pcDNA3.1-IRF7 plasmid, and then 1 μg poly(I:C) stimulation was given after 24 hours. Cells were collected after 3 hours and the expression of *IRF7* (A), *IL28RA* (B), *IL28A* (C), *IL28B* (D) was detected via RT-qPCR. Cell experiments at each time point, n=3. The data are expressed as mean ± s.e.m. NS, not significant, *P < 0.05. Unpaired two-tailed student's t-test (A), and two-way ANOVA with Holm-Sidak's multiple comparisons test (B-D).. Supplemental Figure 6. IL-28A can upregulate the expression of Muc2, Occludin, β-catenin, and E-cadherin. Recombinant IL-28A protein was utilized to stimulate HCT116 for a duration of 24 hours. Following cell harvesting, RT-qPCR was performed to measure intestinal epithelial barrier-related gene expression. *MUC1* (A), *MUC2* (B), *MUC3* (C), *MUC4* (D), *CDH1* (E), *CTNNB1* (F), *OCLN* (G), *CLDN1* (H), *CLDN2* (I), *CLDN3* (J), *CLDN4* (K), *CLDN5* (L), *CLDN11* (M), *TJP1* (N), *DESMOCOLLIN1* (O), *DESMOCOLLIN2* (P), *DESMOCOLLIN3* (Q), and *DESMOPLAKIN* (R). In (A-S), the data are expressed as mean ± s.e.m. NS, not significant, **P < 0.01, ***P < 0.001. Unpaired two-tailed student's t-test (A-R).. Supplemental Figure 7. IL-28A upregulates the protein levels of Muc2, Occludin, β-catenin, and E-cadherin. Recombinant IL-28A protein was utilized to stimulate HCT116 and Caco2 cells for a duration of 24 hours. Following cell harvesting, Western-blot analysis was conducted to measure the levels of intestinal epithelial barrier-related proteins. (A) Representative images, (B) Muc2, (C) E-cadherin, (D) β-catenin and (E) Occludin protein levels in HCT116 cells. (F) Representative images, (G) Muc2, (H) E-cadherin, (I) β-catenin and (J) Occludin protein levels in Caco2 cells. The data are expressed as mean ± s.e.m. NS, not significant, *P < 0.05, **P < 0.01, ***P < 0.001, ****P < 0.0001. Unpaired two-tailed student's t-test (B-E, G-J). Supplemental Figure 8. IRF7 does not affect the gene expression of IL-28A receptors. WT and *Irf7*$^{-/-}$ mice were administered 3% DSS, and then injected intraperitoneally with IL-28A recombinant protein (2 μg/mice) on day 5. Mice were sacrificed on day 8. (A) *Il10rb* expression; (B) *Ifnlr1* expression. WT+DSS+PBS (n=4), *Irf7*$^{-/-}$ +DSS+PBS (n=5), *Irf7*$^{-/-}$ +DSS+IL-28A (n=5). In A-B, the data are expressed as mean ± s.e.m. NS, not significant. One-way ANOVA with Dunnett's multiple comparisons test (A-B). Supplemental Figure 9. IRF7 inhibits the development of colitis. IRF7 may stimulate the production of IL-28A, which in turn upregulates the expression of Muc2, E-cadherin, β-catenin, and Occludin, thereby promoting the integrity of the epithelial barrier and mitigating intestinal inflammation.

Acknowledgements
We thank Prof. Qin Guo of the Sixth Affiliated Hospital of Sun Yat-sen University for assistance.

Author contributions
FQ and HT performed experiments, data analysis and drafted the manuscript; BW, BX, LS, XX, WH, TH, YL, LH performed part of experiments; ZL and QG designed, supervised the project and revised the manuscript. All authors read and approved the final manuscript.

Funding
This work was supported by funds from National Natural Science Foundation of China (31960163), The Jinggang Scholar Program of Jiangxi Province (QD202205), The Scientific and Technological Innovation Team Project and Key Project of Cardiocerebrovascular Disease of Gannan Medical University (TD2021JC01; XN201906), Jiangxi Provincial Natural Science Foundation (20242BAB26091) (To Zhiping Liu), Science and Technology Planning Project of Jiangxi Provincial Health Commission (SKJP_220210670) (To Bingyu Xie), and the program of Guangdong Provincial Clinical Research Center for Digestive Diseases (2020B1111170004) (To Qin Guo).

Availability of data and materials
Data and material will be made available upon reasonable request.

Declarations

Ethics approval and consent to participate
Animal experiments in this study were carried out in accordance with the recommendations of the institutional animal care and use committee of Gannan Medical University. The protocol was approved by the institutional animal care and use committee of Gannan Medical University. The experiments on human samples in this study were reviewed and approved by the Ethics Committee of the Sixth Affiliated Hospital of Sun Yat-sen University. Informed consent was obtained from all individual participants included in the study.

Consent for publication
The authors affirm that human research participants provided informed consent for publication of the images in Fig. 1B–C.

Competing interests
The authors declare no competing financial interests.

Author details
[1]School of Basic Medicine, Gannan Medical University, Ganzhou, Jiangxi, China. [2]Department of Stomatology, Chifeng Maternity Hospital, Chifeng, Inner Mongolia, China. [3]Department of Gastroenterology, The Sixth-Affiliated Hospital of Sun Yat-Sen University, Guangzhou, Guangdong, China. [4]Biomedical Innovation Center, The Sixth-Affiliated Hospital of Sun Yat-Sen University, Guangzhou, Guangdong, China. [5]Department of Gastroenterology, The First-Affiliated Hospital of Gannan Medical University, Ganzhou, Jiangxi, China. [6]Center for Immunology, Key Laboratory of Prevention and Treatment of Cardiovascular and Cerebrovascular Diseases, Ministry of Education, Gannan Medical University, Ganzhou, Jiangxi, China.

Received: 2 March 2024 Accepted: 2 September 2024
Published online: 06 October 2024

References

1. Ungaro R, Mehandru S, Allen PB, Peyrin-Biroulet L, Colombel JF. Ulcerative colitis. Lancet. 2017;389(10080):1756–70.
2. Nowarski R, Jackson R, Gagliani N, de Zoete MR, Palm NW, Bailis W, et al. Epithelial IL-18 equilibrium controls barrier function in colitis. Cell. 2015;163(6):1444–56.
3. Taniguchi K, Karin M. NF-κB, inflammation, immunity and cancer: coming of age. Nat Rev Immunol. 2018;18(5):309–24.
4. Davé SH, Tilstra JS, Matsuoka K, Li F, Karrasch T, Uno JK, et al. Amelioration of chronic murine colitis by peptide-mediated transduction of the IkappaB kinase inhibitor NEMO binding domain peptide. J Immunol. 2007;179(11):7852–9.
5. Murano M, Maemura K, Hirata I, Toshina K, Nishikawa T, Hamamoto N, et al. Therapeutic effect of intracolonically administered nuclear factor kappa B (p65) antisense oligonucleotide on mouse dextran sulphate sodium (DSS)-induced colitis. Clin Exp Immunol. 2000;120(1):51–8.
6. Wang S, Lin Y, Yuan X, Li F, Guo L, Wu B. REV-ERBα integrates colon clock with experimental colitis through regulation of NF-κB/NLRP3 axis. Nat Commun. 2018;9(1):4246.
7. Honda K, Taniguchi T. IRFs: master regulators of signalling by toll-like receptors and cytosolic pattern-recognition receptors. Nat Rev Immunol. 2006;6(9):644–58.
8. Farlik M, Rapp B, Marie I, Levy DE, Jamieson AM, Decker T. Contribution of a TANK-binding kinase 1-interferon (IFN) regulatory factor 7 pathway to IFN-γ-induced gene expression. Mol Cell Biol. 2012;32(6):1032–43.
9. Odendall C, Dixit E, Stavru F, Bierne H, Franz KM, Durbin AF, et al. Diverse intracellular pathogens activate type III interferon expression from peroxisomes. Nat Immunol. 2014;15(8):717–26.
10. Baños-Lara Mdel R, Harvey L, Mendoza A, Simms D, Chouljenko VN, Wakamatsu N, et al. Impact and regulation of lambda interferon response in human metapneumovirus infection. J Virol. 2015;89(1):730–42.
11. Kotenko SV. IFN-lambdas mediate antiviral protection through a distinct class II cytokine receptor complex. Nat Immunol. 2003;4:69.
12. Li W, Lewis-Antes A, Huang J, Balan M, Kotenko SV. Regulation of apoptosis by type III interferons. Cell Prolif. 2008;41:960.
13. Maher SG. IFNalpha and IFNlambda differ in their antiproliferative effects and duration of JAK/STAT signaling activity. Cancer Biol Ther. 2008;7:1109.
14. McElrath C, Espinosa V, Lin JD, Peng J, Sridhar R, Dutta O, et al. Critical role of interferons in gastrointestinal injury repair. Nat Commun. 2021;12(1):2624.
15. Mahlakoiv T, Hernandez P, Gronke K, Diefenbach A, Staeheli P. Leukocyte-derived IFN-alpha/beta and epithelial IFN-lambda constitute a compartmentalized mucosal defense system that restricts enteric virus infections. PLoS Pathog. 2015. https://doi.org/10.1371/journal.ppat.1004782.
16. Pott J. IFN-{lambda} determines the intestinal epithelial antiviral host defense. Proc Natl Acad Sci USA. 2011;108:7944.
17. Schneider WM, Chevillotte MD, Rice CM. Interferon-stimulated genes: a complex web of host defenses. Annu Rev Immunol. 2014;32:513–45.
18. Wu J, Chen ZJ. Innate immune sensing and signaling of cytosolic nucleic acids. Annu Rev Immunol. 2014;32:461–88.
19. Au WC, Moore PA, LaFleur DW, Tombal B, Pitha PM. Characterization of the interferon regulatory factor-7 and its potential role in the transcription activation of interferon A genes. J Biol Chem. 1998;273(44):29210–7.
20. Honda K, Yanai H, Negishi H, Asagiri M, Sato M, Mizutani T, et al. IRF-7 is the master regulator of type-I interferon-dependent immune responses. Nature. 2005;434(7034):772–7.
21. Senatus L, López-Díez R, Egaña-Gorroño L, Liu J, Hu J, Daffu G, et al. RAGE impairs murine diabetic atherosclerosis regression and implicates IRF7 in macrophage inflammation and cholesterol metabolism. JCI insight. 2020. https://doi.org/10.1172/jci.insight.137289.
22. Minaga K, Watanabe T, Arai Y, Shiokawa M, Hara A, Yoshikawa T, et al. Activation of interferon regulatory factor 7 in plasmacytoid dendritic cells promotes experimental autoimmune pancreatitis. J Gastroenterol. 2020;55(5):565–76.
23. Kuroda M, Nishiguchi M, Ugawa N, Ishikawa E, Kawabata Y, Okamoto S, et al. Interferon regulatory factor 7 mediates obesity-associated MCP-1 transcription. PLoS ONE. 2020;15(5): e0233390.
24. Li Y, Wang C, Wu X, Tian H, Jiang S, Xu T, et al. IRF3 and IRF7 contribute to diesel exhaust particles-induced pulmonary inflammation by mediating mTORC1 activation and restraining autophagy in mice. Eur J Immunol. 2020;50(8):1142–53.
25. Negishi H, Miki S, Sarashina H, Taguchi-Atarashi N, Nakajima A, Matsuki K, et al. Essential contribution of IRF3 to intestinal homeostasis and microbiota-mediated Tslp gene induction. Proc Natl Acad Sci USA. 2012;109(51):21016–21.
26. Zaki MH, Vogel P, Malireddi RK, Body-Malapel M, Anand PK, Bertin J, et al. The NOD-like receptor NLRP12 attenuates colon inflammation and tumorigenesis. Cancer Cell. 2011;20(5):649–60.

27. Gurung P, Malireddi RK, Anand PK, Demon D, Vande Walle L, Liu Z, et al. Toll or interleukin-1 receptor (TIR) domain-containing adaptor inducing interferon-beta (TRIF)-mediated caspase-11 protease production integrates toll-like receptor 4 (TLR4) protein- and Nlrp3 inflammasome-mediated host defense against enteropathogens. J Biol Chem. 2012;287(41):34474–83.
28. Platanitis E, Decker T. Regulatory networks involving STATs, IRFs, and NFκB in inflammation. Front Immunol. 2018;9:2542.
29. Turpin W, Lee SH, Raygoza Garay JA, Madsen KL, Meddings JB, Bedrani L, et al. Increased intestinal permeability is associated with later development of Crohn's disease. Gastroenterology. 2020;159(6):2092-100 e5.
30. Mehandru S, Colombel JF. The intestinal barrier, an arbitrator turned provocateur in IBD. Nat Rev Gastroenterol Hepatol. 2021;18(2):83–4.
31. Lopetuso LR, De Salvo C, Pastorelli L, Rana N, Senkfor HN, Petito V, et al. IL-33 promotes recovery from acute colitis by inducing miR-320 to stimulate epithelial restitution and repair. Proc Natl Acad Sci USA. 2018;115(40):E9362–70.
32. Li L, Zhou C, Li T, Xiao W, Yu M, Yang H. Interleukin-28A maintains the intestinal epithelial barrier function through regulation of claudin-1. Ann Transl Med. 2021;9(5):365.
33. Lazear HM, Nice TJ, Diamond MS. Interferon-λ: immune functions at barrier surfaces and beyond. Immunity. 2015;43(1):15–28.
34. Ahn D, Wickersham M, Riquelme S, Prince A. The effects of IFN-λ on epithelial barrier function contribute to klebsiella pneumoniae ST258 pneumonia. Am J Respir Cell Mol Biol. 2019;60(2):158–66.
35. Antonczyk A, Krist B, Sajek M, Michalska A, Piaszyk-Borychowska A, Plens-Galaska M, et al. Direct inhibition of IRF-dependent transcriptional regulatory mechanisms associated with disease. Front Immunol. 2019;10:1176.
36. Neil JA, Matsuzawa-Ishimoto Y, Kernbauer-Hölzl E, Schuster SL, Sota S, Venzon M, et al. IFN-I and IL-22 mediate protective effects of intestinal viral infection. Nat Microbiol. 2019;4(10):1737–49.
37. Odendall C, Voak AA, Kagan JC. Type III IFNs are commonly induced by bacteria-sensing TLRs and reinforce epithelial barriers during infection. J Immunol. 2017;199(9):3270–9.
38. Jefferies CA. Regulating IRFs in IFN driven disease. Front Immunol. 2019;10:325.
39. Read SA, Wijaya R, Ramezani-Moghadam M, Tay E, Schibeci S, Liddle C, et al. Macrophage coordination of the interferon lambda immune response. Front Immunol. 2019;10:2674.
40. Kim TH, Zhou H. Functional analysis of chicken IRF7 in response to dsRNA analog poly(I:C) by integrating overexpression and knockdown. PLoS ONE. 2015;10(7): e0133450.
41. Windsor JW, Kaplan GG. Evolving epidemiology of IBD. Curr Gastroenterol Rep. 2019;21(8):40.
42. Ananthakrishnan AN, Bernstein CN, Iliopoulos D, Macpherson A, Neurath MF, Ali RAR, et al. Environmental triggers in IBD: a review of progress and evidence. Nat Rev Gastroenterol Hepatol. 2018;15(1):39–49.
43. Nambu R, Muise AM. Advanced understanding of monogenic inflammatory bowel disease. Front Pediatr. 2020;8: 618918.
44. Zhang X, Tong Y, Lyu X, Wang J, Wang Y, Yang R. Prevention and alleviation of dextran sulfate sodium salt-induced inflammatory bowel disease in mice with bacillus subtilis-fermented milk via inhibition of the inflammatory responses and regulation of the intestinal flora. Front Microbiol. 2020;11: 622354.
45. Banfi D, Moro E, Bosi A, Bistoletti M, Cerantola S, Crema F, et al. Impact of microbial metabolites on microbiota-gut-brain axis in inflammatory bowel disease. Int J Mol Sci. 2021;22(4):1623.
46. Deng Y, Guo SL, Li JQ, Xie SS, Zhou YC, Wei B, et al. Interferon regulatory factor 7 inhibits rat vascular smooth muscle cell proliferation and inflammation in monocrotaline-induced pulmonary hypertension. Life Sci. 2021;264: 118709.
47. Chen Z, Gu Q, Chen R. Promotive role of IRF7 in ferroptosis of colonic epithelial cells in ulcerative colitis by the miR-375-3p/SLC11A2 axis. Biomol Biomed. 2023;23(3):437–49.
48. Spann KM, Loh Z, Lynch JP, Ullah A, Zhang V, Baturcam E, et al. IRF-3, IRF-7, and IPS-1 promote host defense against acute human metapneumovirus infection in neonatal mice. Am J Pathol. 2014;184(6):1795–806.
49. del Fresno C, Soulat D, Roth S, Blazek K, Udalova I, Sancho D, et al. Interferon-beta production via Dectin-1-Syk-IRF5 signaling in dendritic cells is crucial for immunity to C. albicans. Immunity. 2013;38(6):1176–86.
50. Sin WX, Yeong JP, Lim TJF, Su IH, Connolly JE, Chin KC. IRF-7 mediates type I IFN responses in endotoxin-challenged mice. Front Immunol. 2020;11:640.
51. Bhalla N, Gardner CL, Downs SN, Dunn M, Sun C, Klimstra WB. Macromolecular synthesis shutoff resistance by myeloid cells is critical to IRF7-dependent systemic interferon alpha/beta induction after alphavirus infection. J Virol. 2019. https://doi.org/10.1128/JVI.00872-19.
52. Tan Y, Guan Y, Sun Y, Zheng C. Correlation of intestinal mucosal healing and tight junction protein expression in ulcerative colitis patients. Am J Med Sci. 2019;357(3):195–204.
53. Yu M, Wang Q, Ma Y, Li L, Yu K, Zhang Z, et al. Aryl hydrocarbon receptor activation modulates intestinal epithelial barrier function by maintaining tight junction integrity. Int J Biol Sci. 2018;14(1):69–77.
54. Li X, Li Q, Xiong B, Chen H, Wang X, Zhang D. Discoidin domain receptor 1(DDR1) promote intestinal barrier disruption in Ulcerative Colitis through tight junction proteins degradation and epithelium apoptosis. Pharmacol Res. 2022. https://doi.org/10.1016/j.phrs.2022.106368.
55. Samak G, Chaudhry Kamaljit K, Gangwar R, Narayanan D, Jaggar Jonathan H, Rao R. Calcium/Ask1/MKK7/JNK2/c-Src signalling cascade mediates disruption of intestinal epithelial tight junctions by dextran sulfate sodium. Biochemical Journal. 2015;465(3):503–15.
56. Zhang Z, Xue Z, Yang H, Zhao F, Liu C, Chen J, et al. Differential effects of EPA and DHA on DSS-induced colitis in mice and possible mechanisms involved. Food Funct. 2021;12(4):1803–17.
57. Mahlakõiv T, Hernandez P, Gronke K, Diefenbach A, Staeheli P. Leukocyte-derived IFN-α/β and epithelial IFN-λ constitute a compartmentalized mucosal defense system that restricts enteric virus infections. PLoS Pathog. 2015;11(4): e1004782.
58. Blazek K, Eames HL, Weiss M, Byrne AJ, Perocheau D, Pease JE, et al. IFN-λ resolves inflammation via suppression of neutrophil infiltration and IL-1β production. J Exp Med. 2015;212(6):845–53.
59. Koltsida O, Hausding M, Stavropoulos A, Koch S, Tzelepis G, Ubel C, et al. IL-28A (IFN-λ2) modulates lung DC function to promote Th1 immune skewing and suppress allergic airway disease. EMBO Mol Med. 2011;3(6):348–61.
60. Xu P, Becker H, Elizalde M, Pierik M, Masclee A, Jonkers D. Interleukin-28A induces epithelial barrier dysfunction in CD patient-derived intestinal organoids. Am J Physiol Gastrointest Liver Physiol. 2021;320(5):G689–99.

Publisher's Note

Springer Nature remains neutral with regard to jurisdictional claims in published maps and institutional affiliations.